Simulated impacts of the South Atlantic Ocean Dipole on summer precipitation at the Guinea Coast

Hyacinth C. Nnamchi · Jianping Li ·
In-Sik Kang · Fred Kucharski

Abstract An intermediate complexity atmospheric general circulation model has been used to investigate the influence of the South Atlantic Ocean (SAO) dipole (SAOD) on summer precipitation over the Guinea Coast of West Africa. Two ensemble integrations in which idealized but realistic SAOD-type sea surface temperature (SST) anomaly is prescribed only in the SAO, and then globally are performed and inter-compared. Consistently, above (below) the average precipitation is simulated over the Guinea Coast during the positive (negative) phase of the SAOD. Comparison of the two set of experiments reveal that in its active years, the SAOD is a dominant mechanism that shapes the spatial character of summer precipitation at the Guinea coast, the global SST variability merely slightly moderate its effects. During the SAOD, cool SST anomaly in the extra-tropical SAO off the Brazil–Uruguay–Argentina coast gives rise to suppressed convection and mass divergence. In turn, the subsidence tends to amplify the sub-tropical arm of anomalous Hadley-type circulation and consequently large scale convection and mass flux convergence in the equatorial Atlantic Ocean/Gulf of Guinea region bordering on the coastal fringes of West Africa. Precipitation is therefore increased at the Guinea Coast.

1 Introduction

As the internal variability of the tropical atmosphere is rather weak, the inter-annual and inter-decadal climate variabilities are often strongly dependent on the surface boundary conditions. Indeed, it has been demonstrated that atmospheric circulation and precipitation in the tropics are nearly insensitive to the initial atmospheric conditions but are greatly determined by the sea surface temperature (SST) boundary forcing (Shukla 1998; Ma and Li 2008; Feng et al. 2011). A number of recent studies indicate the occurrence an opposite SST anomaly (SSTA) mode in the South Atlantic Ocean (SAO) and its possible relevance for climate studies (Venegas et al. 1996, 1997; Haarsma et al. 2003, 2005; Colberg and Reason 2007; Trzaska et al. 2007; Nnamchi et al. 2011).

The aim of this present paper is to examine by the use of an intermediate complexity atmospheric general circulation model (AGCM), the influence of this oceanic mechanism referred to as the SAO dipole (SAOD) on summer precipitation at the Guinea Coast[1] of West Africa. We report

H. C. Nnamchi · J. Li (✉)
State Key Laboratory of Numerical Modelling for Atmospheric
Sciences and Geophysical Fluid Dynamics,
Institute of Atmospheric Physics, Chinese Academy of Sciences,
Beijing, China
e-mail: ljp@lasg.iap.ac.cn

H. C. Nnamchi
Graduate University of the Chinese Academy of Sciences,
Beijing, China

I.-S. Kang
School of Earth and Environmental Sciences,
Seoul National University, Seoul, South Korea

F. Kucharski
Earth System Physics Section, Abdus Salam International Center
for Theoretical Physics, Trieste, Italy

---

[1] Two summertime precipitation regions are often identified over West Africa; the Guinea Coast in the south and the Sahel to the north. The boundary between these two regions lies at about 10°–12°N.

that we are successful in simulating the impacts of the SAOD on the region consistent with recent observational studies (Nnamchi et al. 2011; Nnamchi and Li 2011). We further show that in its active phase the SAOD represents a dominant control on the spatial distribution of summer precipitation anomalies over the Guinea Coast, its influence is merely is moderated by the global SST variability.

Attempts to quantify the possible causes of summer rainfall variability in West Africa—with particular emphasis on the recurrent droughts in the Sahel from the 1950s to the 1980s—have generally focused on two mechanisms: the albedo-precipitation feedback resulting from land cover changes (e.g. Charney et al. 1975; Xue and Shukla 1993; Taylor et al. 2002), and the impacts of global SST variability (e.g. Folland et al. 1986; Giannini et al. 2003; Held et al. 2005). However, in recent years there has been a somewhat growing consensus that although the Sahel precipitation may indeed be sensitive to changes in land surface boundary conditions the major control is the global SST variability (Held et al. 2005; Biasutti et al. 2008; Mohino et al. 2011; Rodríguez-Fonseca et al. 2011).

Accordingly, the role of the global ocean has been investigated in several modelling and observational studies on West African precipitation (for recent reviews see Fontaine et al. 2011; Nnamchi and Li, 2011; Rodríguez-Fonseca et al. 2011). Idealized and perturbed modelling experiments report robust response of the region's summer precipitation to SST variability in tropical ocean basins for instance, in the Atlantic (Fontaine et al. 1998; Vizy and Cook 2001; Giannini et al. 2003; Losada et al. 2012; Joly and Voldoire 2010), Indian (Bader and Latif 2011; Mohino et al. 2011) and Pacific (Joly and Voldoire 2009; Mohino et al. 2011) oceans.

There is equally a somewhat increasing realization—largely motivated by observational analyses—that the extra-tropical latitudes may be of greater significance than was previously thought. For instance, the warming of the surface waters in the eastern Mediterranean Sea has been linked enhanced precipitation over the Sahel (Polo et al. 2008; Fontaine et al. 2009; Fontaine et al. 2011). On the other hand, the warming (cooling) anomalies in the Gulf of Guinea associated with concurrent cooling (warming) in the extra-tropical SAO off the Brazil-Uruguay-Argentina coast characteristic of the SAOD has also been related to enhanced (suppressed) precipitation at the Guinea Coast based on observational analyses (Robertson and Mechoso 2000; Nnamchi and Li 2011, Nnamchi et al. 2011). In this study therefore, we focus on the boreal summer season i.e. the June–July–August–September (JJAS) and explore the capability of numerical models to capture this connection by forcing an intermediate complexity AGCM with idealized but realistic SAOD-type SST variability.

The rest of the paper is presented in three sections. Input datasets, the model and formulation of the numerical experiments are described in Sect. 2. This is followed by the observational relationship between different parts of West Africa and the SAO, model climatology and its comparison with reanalysis datasets in Sect. 3. Also described in this section are the model simulated precipitation, wind and convection anomaly fields. Furthermore, the importance of the comprehensive framework offered by considering the influence of the SAOD/extra-tropical SAO on the Guinea Coast (as opposed to the traditional emphasis on *only* the Gulf of Guinea/Atlantic Niño/equatorial Atlantic) is highlighted through discussions of the impact of the SWP-only SSTA as well as the mass flux, moisture transport and Hadley-type circulation associated with the SAO SST variability. In Sect. 4, we present concluding remarks along with some discussions.

2 Data, model and experimental design

2.1 Data and methods

2.1.1 Datasets

This work is largely based on idealized AGCM simulation experiments in which the model is forced with SAOD-type SSTA derived from the National Oceanic Atmospheric Administration (NOAA) Extended Reconstructed SST (NOAA ERSST) version 3b available at 2° longitude by 2° latitude horizontal grids (Smith et al. 2008) for the period 1950–2010. Other model input boundary conditions have been derived from the European Centre for Medium-Range Weather Forecast's ERA-Interim reanalysis (Dee et al. 2011).

The University of Delaware monthly precipitation dataset at $0.5° \times 0.5°$ for 1950–2008 was also used to first highlight the observed relation of West African precipitation to the SAO SST variability. For each of the SST and precipitation datasets, monthly anomalies were computed by subtracting the climatological mean from the individual monthly means. The datasets are then averaged for the JJAS season.

2.1.2 SAOD and precipitation indices

An indicator of dipole events is the SAOD index (SAODI). The SAODI is the basis for constructing SSTA composite fields used as the lower SSTA boundary conditions for the AGCM sensitivity experiments. Following Nnamchi et al. (2011), the SAODI is defined by calculating the difference between the domain-averaged SSTA of the two centres of action associated with the dipole, viz:

$$SAODI = [SSTA]_{NEP} - [SSTA]_{SWP} \qquad (1)$$

where the square brackets indicate domain averages, the subscripts show the area over which the SSTA averages are computed. These domains are the northeast pole (NEP: 10°E–20°W, 0°–15°S) and the southwest pole (SWP: 10°–40°W, 25–40°S). These domains as the well as the Atlantic Niño region are shown in Fig. 1a.

Precipitation indices for West Africa and parts thereof are used to investigate connections with the SAOD by regression analysis. Following Janowiak (1988), the domain-averaged precipitation for the Guinea Coast, Sahel and the entire West African region are used as the indices for the respective regions. These three domains are determined as shown in Fig. 1b.

2.1.3 SAOD, Atlantic Niño and determination of the SST anomaly composites

From Fig. 1a we see that the NEP region falls within the Atlantic Niño domain, and as shown by Nnamchi and Li
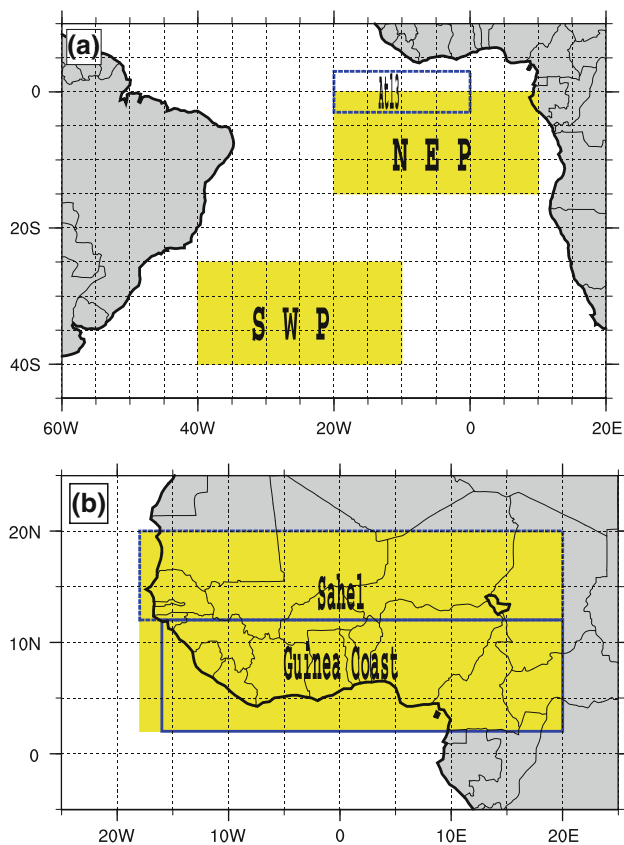
Fig. 1 a Domains for determining the SAOD namely the North-East Pole (NEP), South-West Pole (SWP) and the Atlantic Niño (Atl3). These are defined as follows; NEP: 10°E–20°W, 0°–15°S; SWP: 10°–40°W, 25°–40°S (Nnamchi et al. 2011) and Atl3: 0°–20°W, 3°N–3°S (Zebiak 1993). **b** Domains over which the Guinea Coast (20°E–15°W, 2°–10°N), the Sahel (20°E–20°W, 10°–20°N) and West African (20°E–18°W, 2°–20°N) precipitation indices are averaged, modified from Janowiak (1988)

(2011) these the two indices are strongly correlated. Yet, not all Atlantic Niño cases co-occur with significant SSTA over the SWP in the extra-tropics. Thus, SAO SSTA response to the Atlantic Niño is characterized by domain-scale homogenous and generally statistically significant warming with maximum anomalies in the equatorial Atlantic Ocean (Fig. 2a). Conversely, SSTA response to the SAOD features significant warming over the equatorial region and cooling in the extra-tropics. The implication of the spatial patterns of the two phenomena is that the value of the SAODI could be unduly influenced by the equatorial variability: strong warming (cooling) over the NEP only characteristic of the classical Atlantic Niño means high (low) SAODI value even if there is no marked SST variability at the SWP.

Therefore, in order to objectively composite the positive SAOD years for the AGCM experiments, we chose only those SAOD years in which pronounced cooling actually occurred in the SWP. This is determined as those years in which the normalized value of the SAODI is +0.75 or greater and the SWP index is −0.5 or less (Fig. 3a). By putting the SWP variability into account, we ensure that those high SAODI values caused by the classical Atlantic Niño i.e. when there is no cooling in the extra-tropics are not treated as dipole events. This way eight (8) years namely 1951, 1963, 1964, 1968, 1974, 1996, 1998 and 1999 are identified as positive dipole years.

Another important consideration is the possible roles played by the equatorial Pacific Ocean based El Niño in determining the influence of the impacts of the SAOD on Guinea Coast precipitation. Figure 3b demonstrates that of the eight cases of SAOD used, four (i.e. 1951, 1968, 1974 and 1998) are El Niño years; the other 4 years (1964, 1974, 1996 and 1999) are La Niña years—defined by the index value of greater or less than zero. However, it is important to note that: (i) the El Niño/La Niña SST amplitudes are generally weak, and (ii) the co-occurrence of the SAOD positive phase with both equatorial Pacific warming and cooling means that when the data is averaged over the above 8 years, the otherwise weak El Niño/La Niño SSTAs cancel each other (Fig. 4). The Niño 3 index is neither correlated with the SAODI (r = −0.16) nor with Guinea Coast summer precipitation (r = −0.003).

2.2 Model

Idealized numerical experiments have been designed and implemented on the Simplified Parameterizations, primitivE-Equation DYnamics (SPEEDY) model developed at the Abdus Salam International Centre for Theoretical Physics, Trieste, Italy (Molteni 2003; Kucharski et al. 2006). SPEEDY is an intermediate complexity AGCM based on a spectral primitive-equation dynamical core
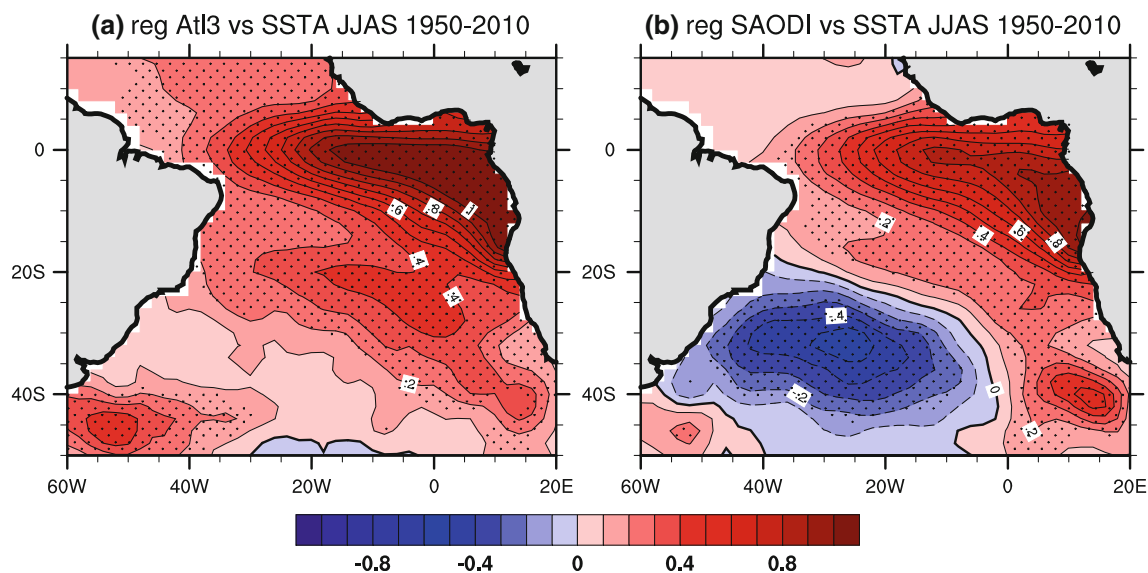
Fig. 2 South Atlantic Ocean SSTA response to **a** Atlantic Niño and **b** SAOD determined by regression analysis. Grid points for which regression coefficients are significant at 95 % confidence level are dotted
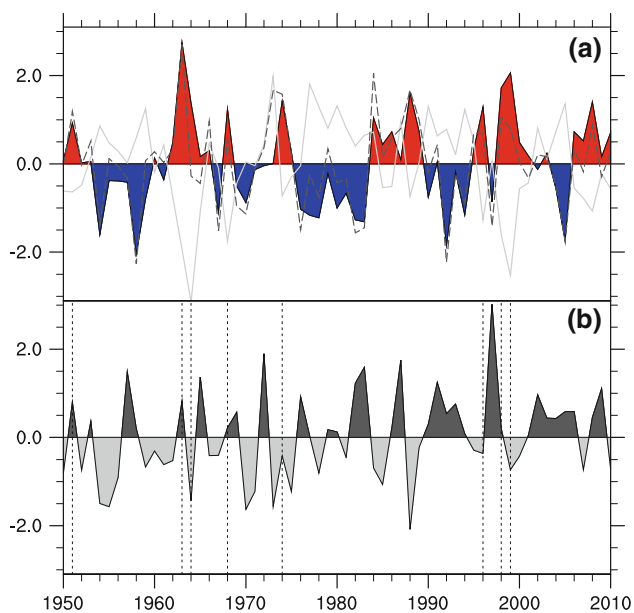
Fig. 3 **a** Normalized indices of the SAOD (*colourfill*), SWP (*solid line*) and NEP (*dashed line*). **b** Niño 3 index for the corresponding period. *Dotted vertical lines* indicate dipole years determined by SAOD index of +0.75 or greater and SWP of −0.5 or less. The SAOD years are 1951, 1963, 1964, 1968, 1974, 1996, 1998 and 1999

(Held and Suarez 1994), with a hydrostatic, σ-coordinate, spectral transform (Bourke 1974) and semi-implicit treatment of gravity waves.

There are eight σ- levels and standard horizontal resolution corresponding triangular truncation at total wave number 30 (T30), standard Gaussian grids of 96 by 48 points and a suit of simplified parameterization schemes. The parameterized processes include convection,

large-scale condensation, clouds, radiation (short- and long- wave), vertical diffusion, and surface momentum and energy fluxes. Despite the parameterizations, the quality of the SPEEDY simulated climates compares very well with those of the more complex AGCMs, and there are several recent applications of the model in similar studies (e.g. King et al. 2010; Bulic and Kucharski 2012; Kucharski et al. 2011; Molteni et al. 2011; Zamboni et al. 2012). Information is available on the earlier/latest versions of SPEEDY, its users, how to access the model and assessment of its performance, at the following web-page: http://www.ictp.it/∼kucharsk/speedy-net.html.

2.3 Experimental design

We report the results of eight simulations using the SPEEDY AGCM forced with the JJAS averaged SST datasets. These experiments are summarized in Table 1 and are described below:

(i) *Control:* a 61-ensemble integration forced with the JJAS averaged climatological SST. The output provides the basic JJAS climatological dataset against which we evaluate the relative significance of idealizing the SSTA in subsequent sensitivity experiments.

(ii) *Positive SAOD-only experiment:* a 61-ensemble integration in which the AGCM is forced with JJAS SAOD-type SSTA composite imposed on the climatological SST only in the SAO region (10°N–45°S, 20°E–60°W). Outside this domain, the climatological SST is prescribed. The SSTA pattern is shown Fig. 4a. The SSTA is characteristic of the positive

Fig. 4 Imposed SSTA for the SPEEDY AGCM Experiments (contour interval 0.2 K). **a** SSTA for the SAOD-only experiments and **b** SSTA for the SAOD + Global SSTA experiments. *Thick black contour* represent 0 K; dashed contours indicate negative SSTA, *solid contours* indicate positive values
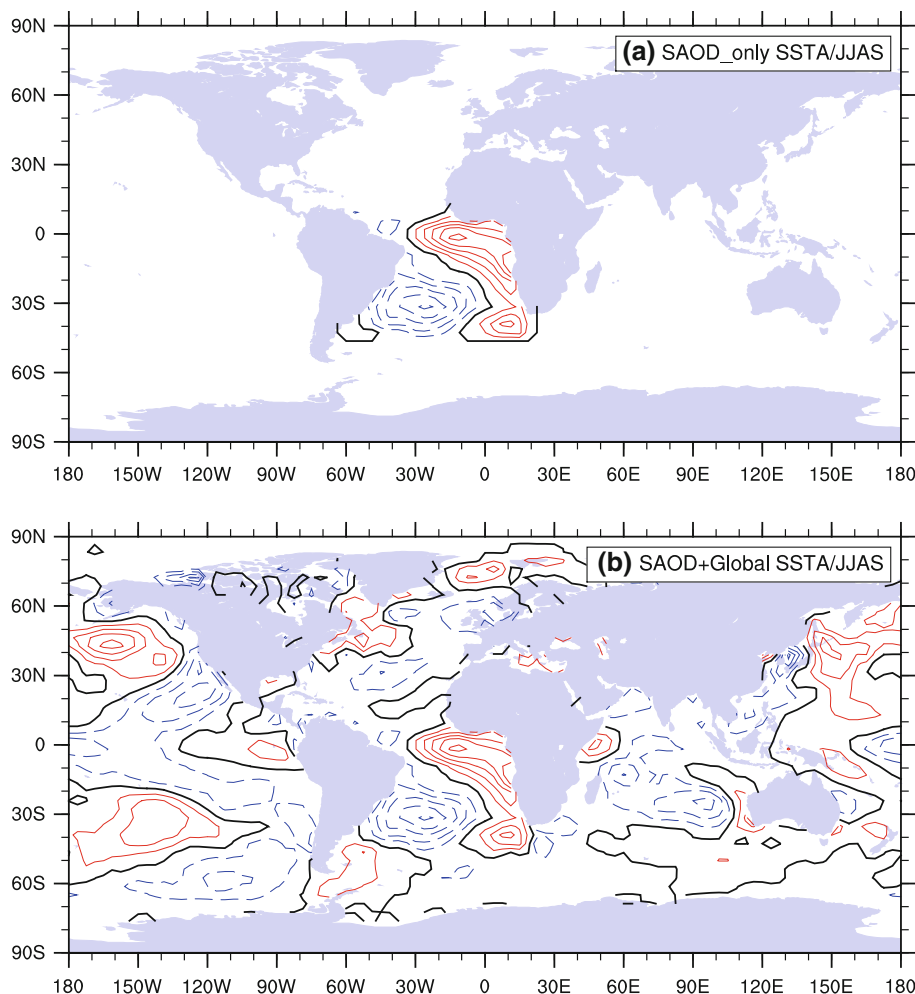
Table 1 Basic information on the numerical experiments performed

| SN	Experiment	Domain[a]	Ens[b]
1.	Control	Global ocean	61
2.	Positive SAOD-only	10°N–445°S, 20°E–60°W	61
3.	Negative SAOD-only	10°N–445°S, 20°E–60°W	61
4.	Positive SAOD + global SSTA	Global Ocean	61
5.	Negative SAOD + global SSTA	Global Ocean	61
6.	Global SSTA without SAOD	Global ocean, except 10°N–45°S, 20°E–60°W	61
7.	NEP-only	10°N–445°S, 20°E–60°W	61
8.	SWP-only	10°N–445°S, 20°E–60°W	61

[a] Refers to the region in which the JJAS-averaged SSTA composite is imposed on the climatological SST, and outside which the model is forced with only climatological SST

[b] Ens is the number of ensembles of the integration

phase of the SAOD, with warming in the NEP and cooling in the SWP region. By restricting the SSTA to the SAO only, we aim to identify the impacts of the

SAOD in its active years without the external influence of the global SST variability.

(iii) *Negative SAOD-only experiment:* Same as experiment (ii) above, but the SSTA is inversed by multiplying with by −1. By inversing the SAOD SSTA, we aim to use this experiment to establish if opposite effect on the Guinea Coast JJAS precipitation could be produced. We have used the same composite (instead of extracting negative SAOD-type SSTA directly from data) to provide an immediate and direct sense of comparison with the results of the *positive SAOD-only experiment*.

(iv) *Positive SAOD + global SSTA experiment:* a 61-ensemble integration in which the AGCM is forced with JJAS global SAOD-type SSTA composite as shown in Fig. 4b. By extending the SSTA beyond the SAO, our aim is to show the additional contributions of global SSTA to the Guinea JJAS precipitation during the active phase of the SAOD.

(v) *Negative SAOD + global SSTA experiment:* Same as experiment (iv) above, but the SSTA is inversed by
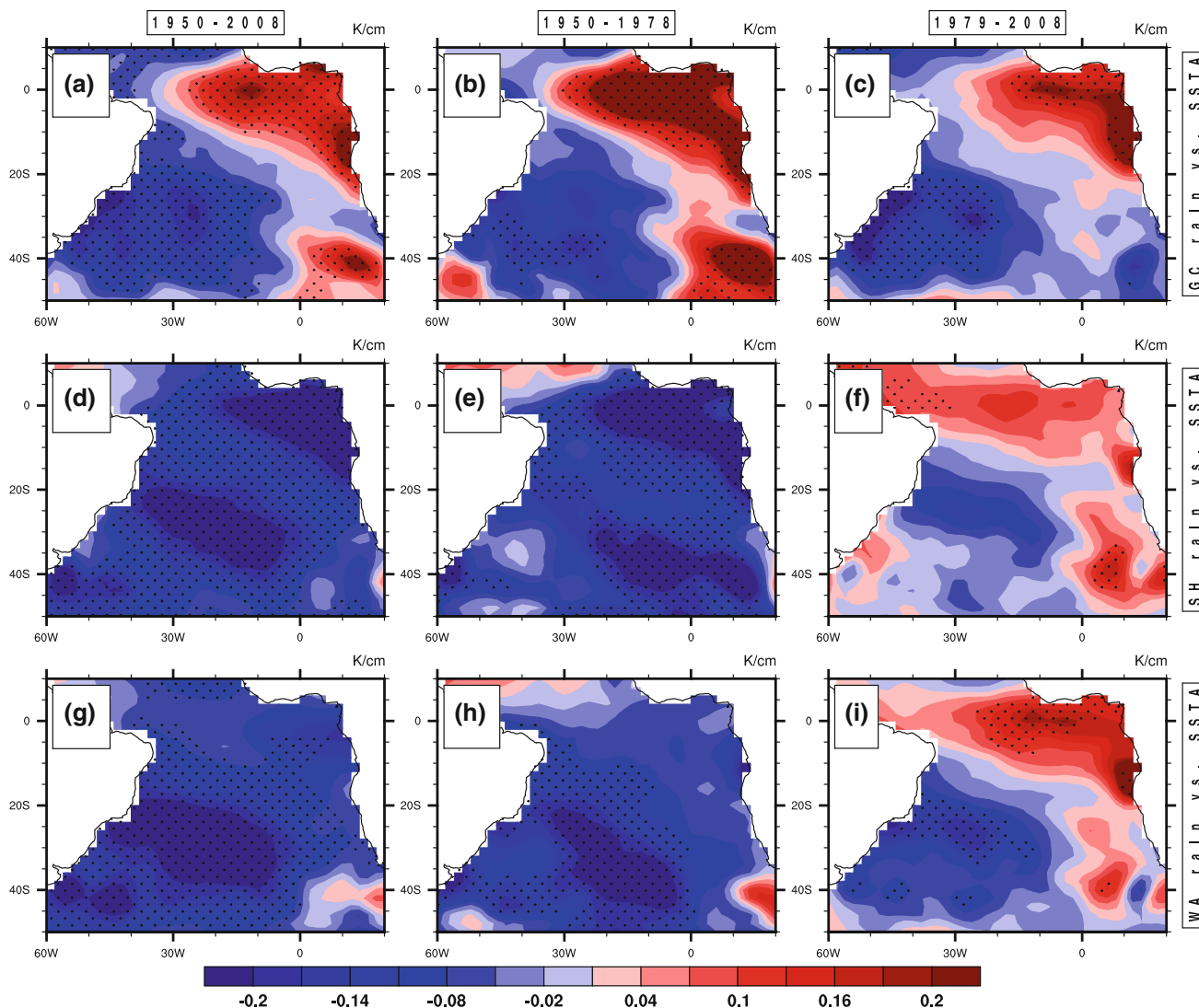
Fig. 5 Observed SSTA regressed onto Guinea Coast (**a–c**), Sahel (**d–f**) and West African (**g–i**) precipitation indices for 1950–2008 (*left panels*), 1950–1978 (*middle panels*) and 1979–2008 (*right panels*).

See Fig. 1b for the definition of the indices. *Dots indicate* regressions significant at 95 % confidence level. The contour interval is 0.03 K/cm

multiplying it by −1 to ascertain the opposite effect on precipitation over the Guinea Coast.

(vi) *Global SSTA without SAOD:* a 61-ensemble integration of the AGCM in which the climatological SST is prescribed in the SAO domain. Elsewhere the observed SSTA composite is imposed on the climatology. Although the SAO SSTA may contain signal of the global SST variability, from Fig. 4 it is quite obvious that the SAOD represents the dominant pattern over the region in its active years. Therefore, the aim of this experiment is to identify the effects of the global SST variability of Guinea Coast precipitation in such years in absence of the dominant SAOD pattern.

(vii) *NEP-only experiment:* a 61-ensemble integration in which the AGCM is forced with the JJAS NEP-type

warm SSTA composite (only positive values in Fig. 4a). Elsewhere the climatological SST is prescribed. The aim of this experiment is to reproduce the well-known response of Guinea Coast precipitation to the NEP/Gulf of Guinea/Atlantic Niño region for comparison with the SAOD- and SWP-only experiments.

(viii) *SWP-only experiment:* a 61-ensemble integration in which the AGCM is forced with the JJAS SWP-type cool SSTA composite (only negative values in Fig. 4a). Elsewhere including over the NEP, the climatological SST is prescribed. The aim of this experiment is to see how the Guinea Coast precipitation field responds to cooling in the SWP region only, in absence of the global SSTA and without warming at the NEP.
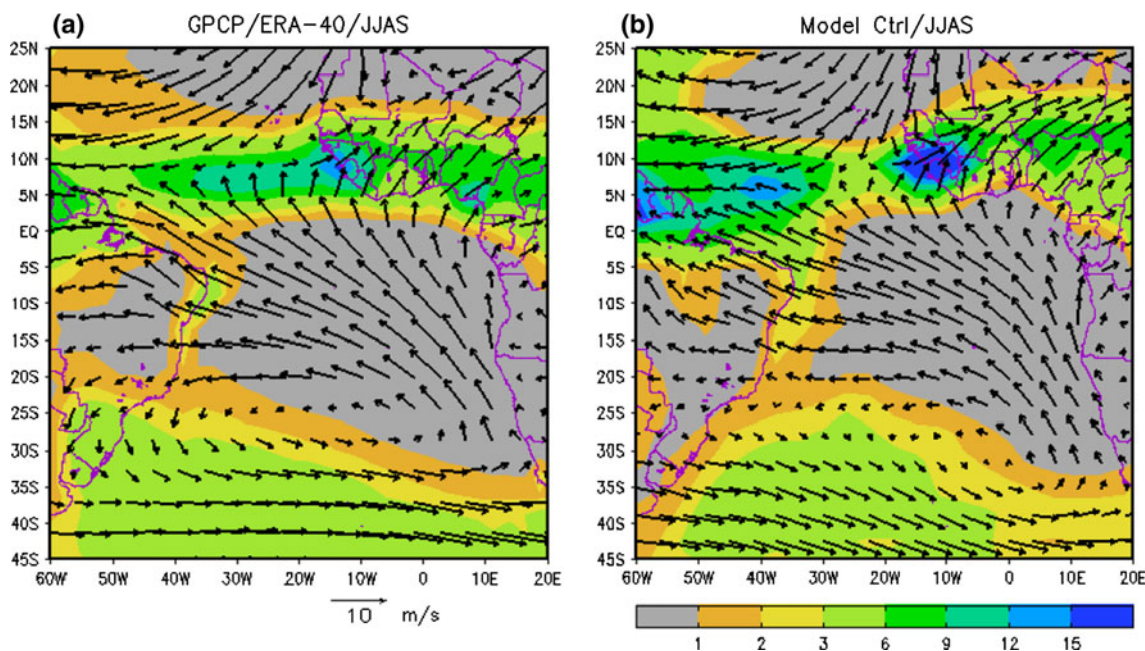
Fig. 6 a GPCP precipitation (shading: unit, mm day^{-1}) and ERA-40 925 hPa winds in m s^{-1} for JJAS. **b** Same as (**a**) but as simulated in the SPEEDY AGCM *control experiment*

The NEP roughly falls within the same domain as the classical Atlantic Niño which has long been known to influence Guinea Coast summer precipitation (Wagner and Da Silva 1994; Vizy and Cook 2001). Therefore, although the NEP and SWP anomalies co-occur during the SAOD events, we hope to learn from this idealized experiment if any relationship exists between the SWP and precipitation over Guinea Coast in absence of the NEP.

In the following discussions, the plots have been created by computing the grid-point difference between the climatological and sensitivity experiments, or between the positive and negative experiments and then taking the average. Given any parameter P, anomaly with respect to the climatological simulation is calculated as follows:

$$\Delta P = A_{EXPT} - CLM \tag{2}$$

where A_{EXPT} is the sensitivity experiment under consideration; CLM is the climatological experiment. On the other hand, when positive (POS_{EXPT}) and negative (NEG_{EXPT}) experiments are used for one plot, we have:

$$\Delta P = \frac{POS_{EXPT} - NEG_{EXPT}}{2} \tag{3}$$

Thus, the anomalies are characteristic of the positive phase of the SAOD. In all cases, the first year of integration has been excluded from the analysis as the model spin-off before the anomalies are fully developed.

3 Results

3.1 Observed relationship between West African summer precipitation and SAO SST variability

We first highlight the observed relationship between West African precipitation anomalies and SAO SST variability. The boundary between the Guinea Coast and the Sahel is often drawn along latitudes 10°–12°N. Therefore, as shown earlier in Fig. 1b we define three precipitation indices to represent summer precipitation for the Guinea Coast, Sahel and the entire West African region.

Figure 5a show that the regression of the Guinea Coast precipitation index produces a clearly defined dipole with statistically significant coefficients of opposite signs over the NEP and SWP for the entire 1950–2008 period. To explore the stability of the regression, we divided the datasets into two epochs of roughly equal length, and the results show that SAOD SSTA-type is the dominant pattern of the SAO relations to the Guinea Coast precipitation in both the 1950–1978 (Fig. 5b) and 1979–2008 (Fig. 5c) periods. On the other hand, the Sahel precipitation is linked to domain-wide cooling with centres in the Atlantic Niño region as well as over the SWP during the entire study period (Fig. 5d). However, this relationship is not stationary in time as the SWP cooling is weaker during the first epoch (1950–1978) but the pattern becomes SAOD-like during the last 30 years (Fig. 5e–f).
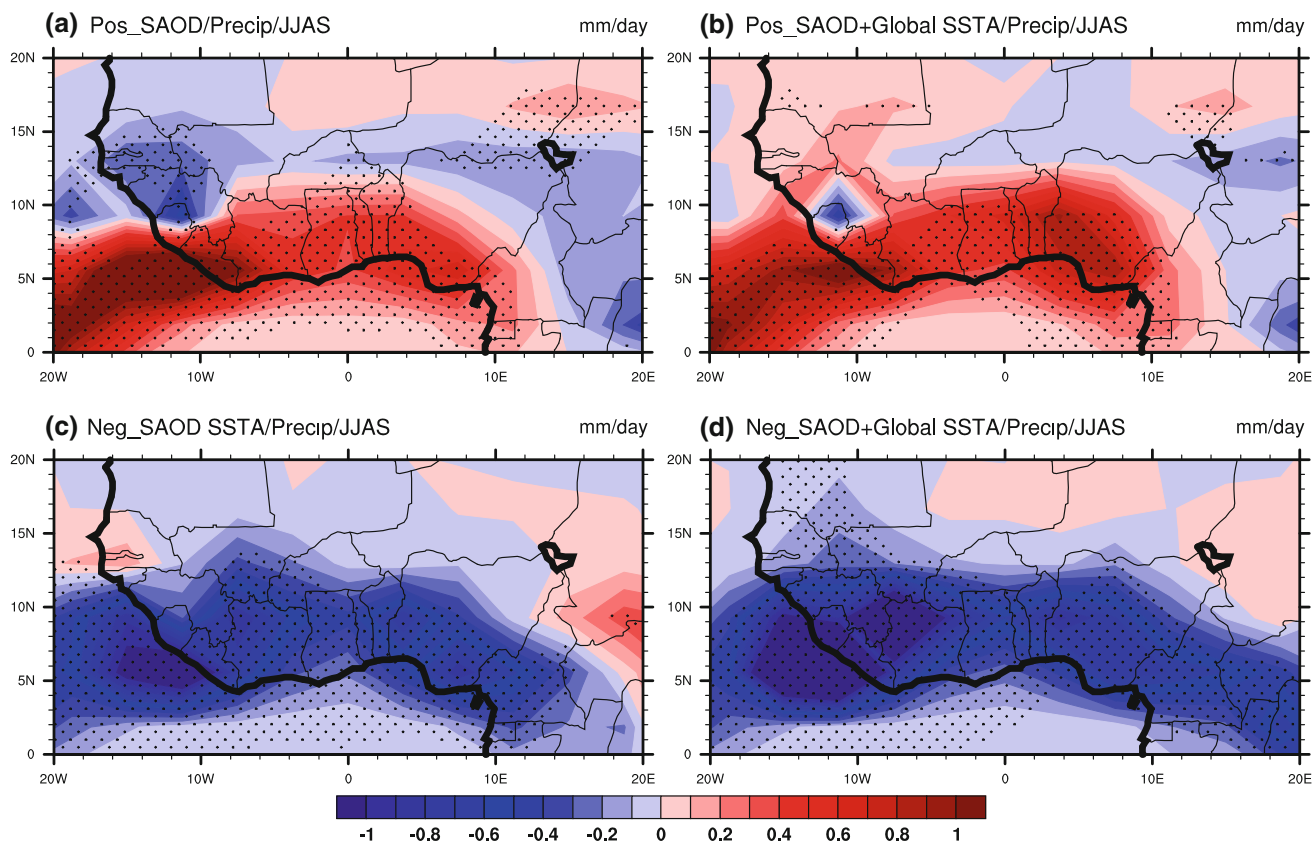
Fig. 7 Precipitation anomalies over the Guinea Coast during the positive phase of the SAOD for **a** *SAOD-only experiment* and **b** *SAOD + global SSTA experiment*. **c**, **d**, the same as (**a**, **b**), but for the negative phase of the SAOD. *Dots* indicate significant precipitation anomalies at 95 % confidence level

For the entire West Africa, strong (comparatively weak) responses are found in the SWP (NEP) region for the 1950–2008 period (Fig. 5g). Considered on the basis of the two epochs, the NEP SSTA response is practically undetectable during the 1950–1978 period but a phase shift characterized by SAOD pattern is witnessed during the latter epoch (1979–2008). A comparison of the six panels of Fig. 5 suggests that while the relationship between the Guinea Coast precipitation and SAO SST variability is a stable dipole pattern throughout the study period, for the entire West African region the connection is unstable which is largely attributable to the Sahel variability.

## 3.2 Model circulation and precipitation climatology

How well the AGCM simulates the JJAS climatological climate is examined in this section by comparing the control integration with reanalysis datasets. Figure 6 shows the Global Precipitation Climatology Project (GPCP) precipitation (Adler et al. 2003) and the European Centre for Medium-Range Weather Forecast's 40-year reanalysis (ERA-40) 925 hPa horizontal winds (Uppala et al. 2005), and the SPEEDY control simulation of the same parameters.

Figure 6 shows that the SPEEDY effectively captures the large scale patterns of the observed precipitation and near surface winds in the SAO—West African region. Also the model efficiently reproduces the major dynamical features including the SAO sub-tropical anticyclone, the equatorial and monsoon circulations. A notable bias is that the simulated 1 mm contour hinges on the Guinea Coast, but is further south over the ocean in the GPCP dataset. Again the model simulated 16 mm contour over the Guinea highlands in the western part of West Africa is more extensive compared to the GPCP dataset.

However, it is important to note that all the plots in Fig. 6 do not refer to exactly the same period; the SPEEDY run is based on 1950–2010 climatological SST, the GPCP precipitation dataset is for 1979–2008 while the ERA-40 covers the period 1958–2000. As has been highlighted elsewhere (e.g. De Xue et al. 2010; Kucharski et al. 2011), the model biases indicated are essentially typical of most AGCMs, and in the case the SPEEDY could be attributable to several factors such as the low (horizontal and vertical) resolutions and deficiencies in the convection and surface-flux parameterizations schemes. To minimize the effects of these biases on the results presented here, we have

Fig. 8 Relative impacts of the SAOD and global SST variability on Guinea Coast precipitation (determined by *SAOD + global SSTA* minus *SAOD-only* simulated precipitation) in positive (*upper panel*) and negative (*lower panel*) phases of the SAOD. *Dots* indicate significant precipitation anomalies at 95 % confidence level
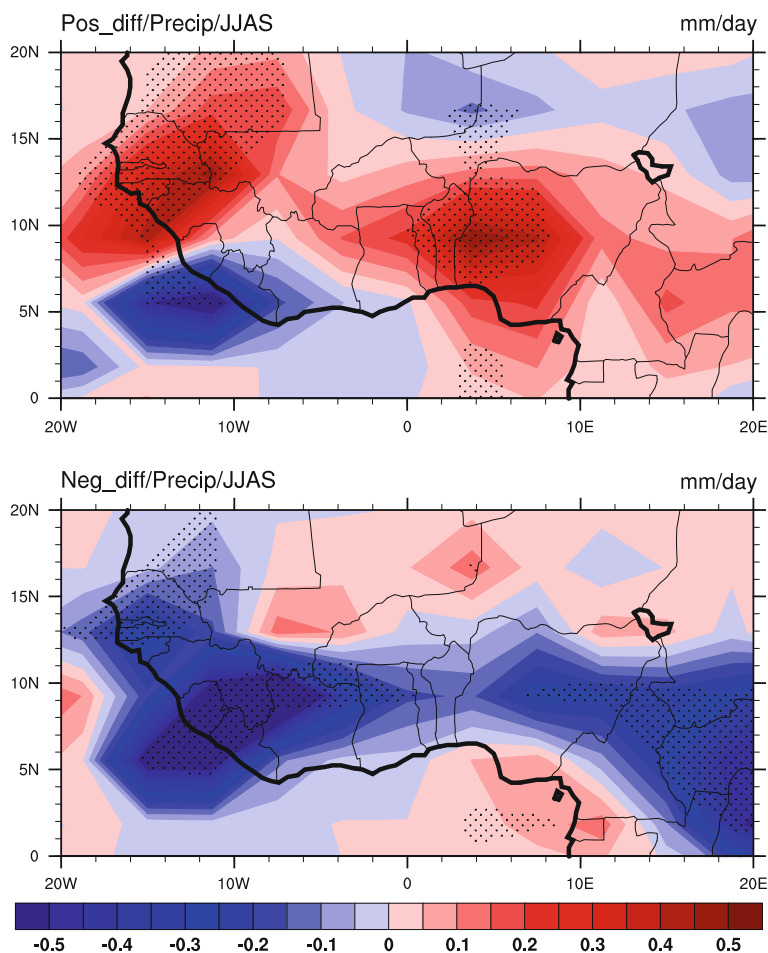
Fig. 9 Guinea Coast precipitation simulated in the *global SSTA-only experiment*, with climatological SSTA prescribed in the South Atlantic Ocean. *Dots* indicate significant precipitation anomalies at 95 % confidence level
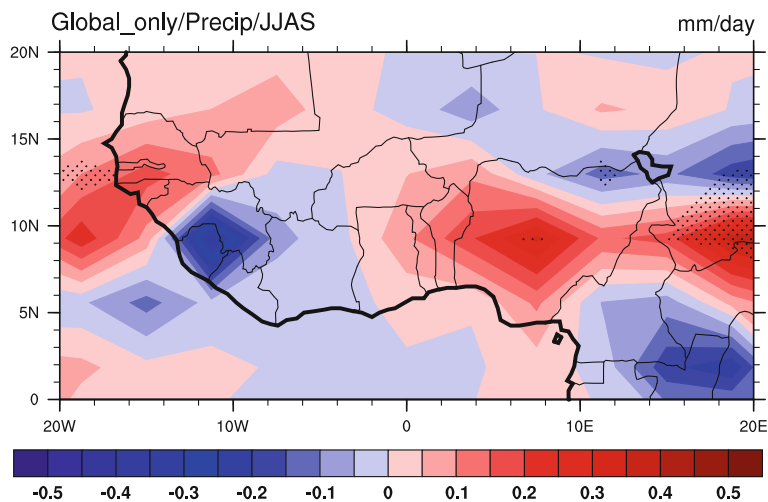
conducted all the experiments in this study over the same length of integration using input datasets derived over the same period. Thus, by comparing the climatologies of the different sensitivity experiments and/or with the control run we hope to elicit useful information on how the SAOD could affect Guinea Coast precipitation.

3.3 Precipitation and circulation anomalies associated with the SAOD

In this section, we describe the Guinea Coast precipitation anomalies during the SAOD and the associated winds, extending further afield into the SAO. As shown in Fig. 7a,
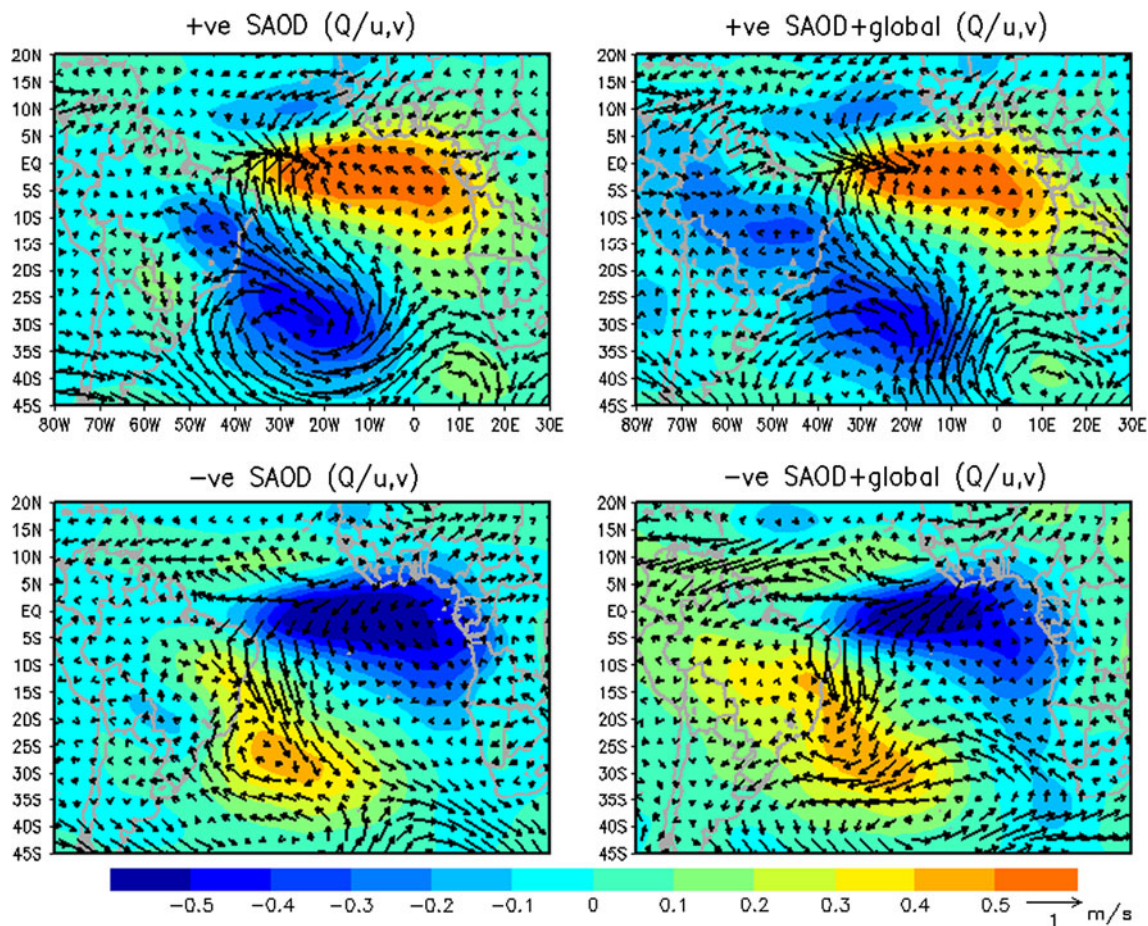
Fig. 10 Specific humidity (shading, in g kg^{-1}) and 925-hPa winds (vector, in m s^{-1}) associated with the SAOD

the *positive SAOD-only* SSTA is associated with three major precipitation anomaly patterns over West Africa. One is a large area in the Guinea Coast (south of 11°N and west of 15°E) with pronounced, statistically significant increase in precipitation; two, in the mid-belt and eastern parts there is reduced precipitation that is significant only in the western part and three, in the northern extremity there is increase in precipitation, although of far smaller magnitude and generally statistically insignificant. Similar large area of homogenous precipitation significant increase is also well reproduced over the Guinea coast in the *SAOD + global SSTA experiment* as shown Fig. 7b. Elsewhere over West Africa, the magnitudes of the anomalies are comparatively low and insignificant.

Figure 7c, d shows that the negative phase of the SAOD is equally associated with widespread failure of rainfall extending well into the Sahel, although statistically significant mainly over the Guinea Coast. Interestingly, the simulated response of precipitation is more homogenous and of larger magnitude in the negative phase of the SAOD compared to the positive phase. In the northeastern parts of the domain, there is a very weak increase in precipitation in

both the *SAOD-only experiment*, which disappears in the *SAOD + global SSTA experiment* (Fig. 7d).

More importantly, in both the negative and positive phases of the SAOD significant response of precipitation is found over the Guinea Coast region consistent with the previous observational analyses (Nnamchi et al. 2011; Nnamchi and Li, 2011). It is also noteworthy that the precipitation anomalies are basically similar in the *SAOD-only* and *SAOD + global SSTA global* experiments. The discrepancies are mainly in terms of the magnitude of the precipitation anomalies, as is further highlighted by the composite difference between the two sets of experiments in positive and negative phases of the SAOD (Fig. 8). From Fig. 8, it is evident that after subtracting the *SAOD-only experiments* from the *SAOD + global SSTA experiments*, the Guinea Coast is largely characterized by increased (reduced) precipitation anomalies in the positive (negative) phase of the SAOD suggesting that the dominant effect of the SAOD tends to be amplified by the global SST variability.

To investigate the roles of global SST variability further, we implemented an additional integration with the observed SSTA composite imposed over the global ocean,

Fig. 11 Composite average of the OLR (W/m²) associated with the SAOD. The contour interval is 0.2
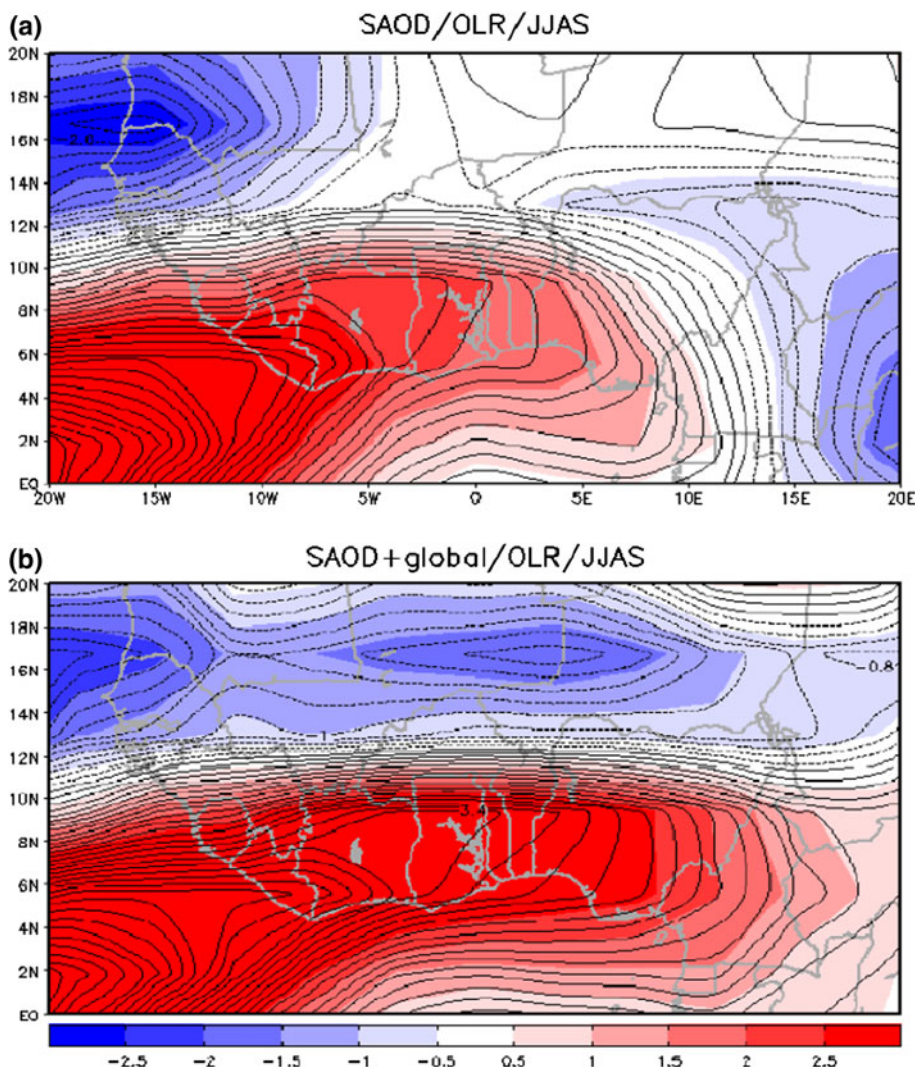
except the SAO where the climatological SST is prescribed—*the global SSTA without experiment*. Figure 9 shows that the model fails to simulate coherent precipitation anomalies over the Guinea Coast, as in the other experiments in which the SAOD is included. Instead, there is pronounced precipitation failure over the Guinea highlands where precipitation increases are most noticeable if the SAOD is included. On the other, strong positive anomalies are simulated over the mid-belt of Nigeria and the Chad-Central African border. Note also that the precipitation response is generally weak and statistically insignificant in the absence of the SAOD-type SSTA. These suggest that in its active years, the SAOD represents a dominant mechanism that controls the spatial pattern of precipitation anomalies at the Guinea Coast, but the global SST variability affect the actual amounts of precipitation received.

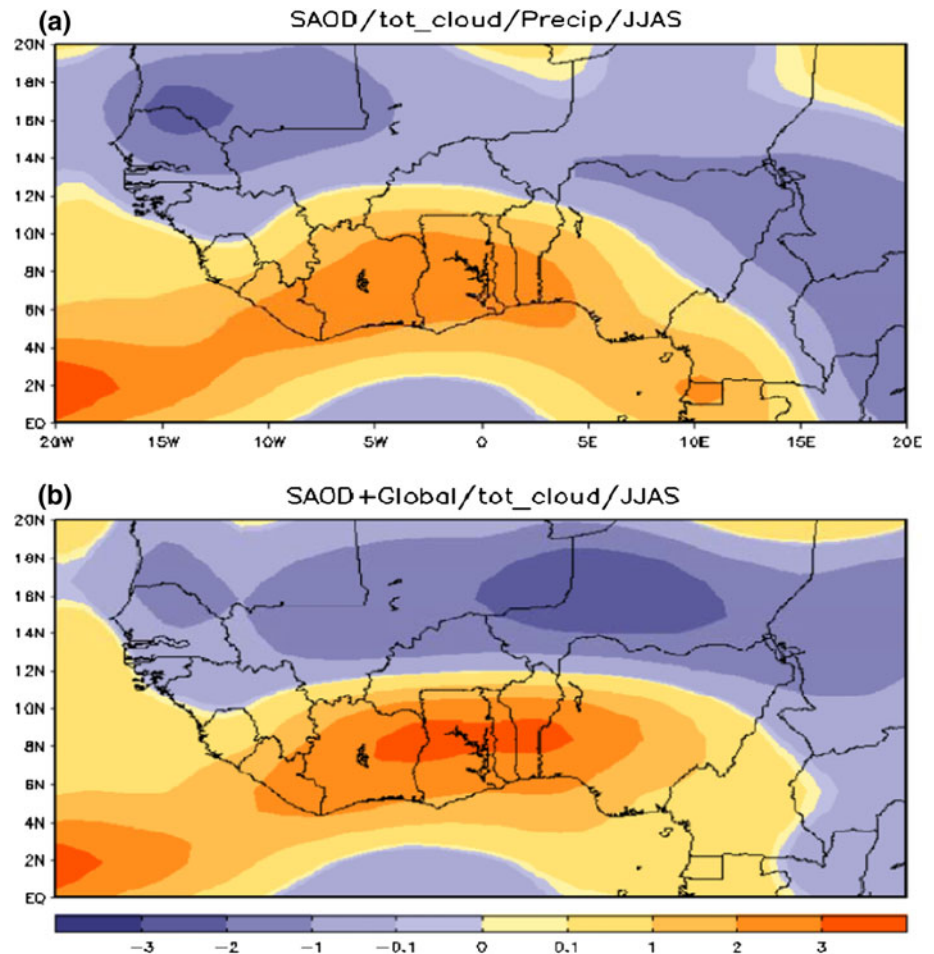Associated with the Guinea Coast precipitation anomaly fields is a strengthening of the SAO sub-tropical anticyclone over the SWP (more clearly defined in the *SAOD-only experiment*) which feeds a cyclonic circulation over NEP in the equatorial belt during the positive phase of the SAOD as revealed by the 925 hPa circulation fields (Fig. 10). The NEP-Guinea region is characterized by surplus of specific humidity indicating the availability of moisture for the enhanced precipitation. In negative phase, these are patterns are reversed thereby suppressing the occurrence of precipitation over the Guinea Coast.

3.4 Convection fields

As it is already shown that the positive (negative) phase of the SAOD is associated with enhanced (suppressed) precipitation over the Guinea we now examine the SAOD-type convection anomalies.

Figure 11 shows the out-going longwave radiation (OLR) over the region as an indicator of atmospheric convection during the SAOD. It is readily evident that the

Fig. 12 Composite average of the total cloudiness (%) at the Guinea Coast associated with the SAOD. The total cloudiness is estimated as the average of deep and stratus clouds

OLR is closely related to the precipitation field. Thus, the Guinea Coast region of homogeneous precipitation anomalies is characterized by enhanced convection with the strongest magnitude over the west coast in the *SAOD-only experiment*. In the northwestern and eastern segments of the domain however, convection is suppressed. Another region of fairly enhanced convective activity occurs over the eastern half of locations north of 16°N. In the *SAOD + global SSTA experiment*, there more is clearly defined south-north dipole in the convection field over West Africa: enhanced convection over the Guinea Coast extends from western to the eastern extremity, while in the Sahel there is a similar west-east pattern but of suppressed convection.

The importance of the SAOD-induced convection anomaly pattern over the Guinea Coast is reflected in the cloud cover (Fig. 12). Thus, there are above the average cloudiness at most locations over the region, but further inland cloudiness drops to below average in the Sahel. These spatial differences in atmospheric convective activity revealed by the OLR vis-à-vis cloudiness explain the spatial differences also in precipitation anomalies described in Sect. 3.3.

3.5 Is the SAOD really important for Guinea Coast precipitation?

A large body of available literature based observational and modelling have since demonstrated that SSTA in the NEP/Gulf of Guinea/Atlantic Niño region affects summer precipitation over the Guinea Coast (Wagner and Da Silva 1994; Vizy and Cook 2001; Giannini et al. 2003; Polo et al. 2008; Losada et al. 2012; Joly and Voldoire 2010). However, observations show that the SAOD is characterized by strong SSTA in the NEP occurring concurrently with another SSTA equally robust, but of opposite sign in the SWP off the Brazil-Uruguay-Argentina coast (cf. Figs. 2b, 4). And, we have seen from the foregoing analyses that this opposite polarity mode is also strongly associated with summer precipitation at the Guinea Coast. The question is now of the form: Does the opposite SSTA mode really affect Guinea Coast precipitation, is the SWP of any significance or is the NEP/Atlantic Niño/Gulf of Guinea on the immediate coast enough to account for the precipitation anomalies?

In order to address the above questions; first, we further idealize the numerical experiment to consider only the

Fig. 13 Precipitation (unit: mm day^{-1}) anomalies simulated in the **a** *NEP-only experiment* forced with only the positive SSTA in Fig. 4a; **b** *SWP-only experiment* forced with only the negative SSTA in Fig. 4a and **c** the SAOD *minus* NEP experiments difference. *Dots* indicate significant precipitation anomalies at 95 % confidence level in (**a**) and (**b**) and 90 % in (**c**)
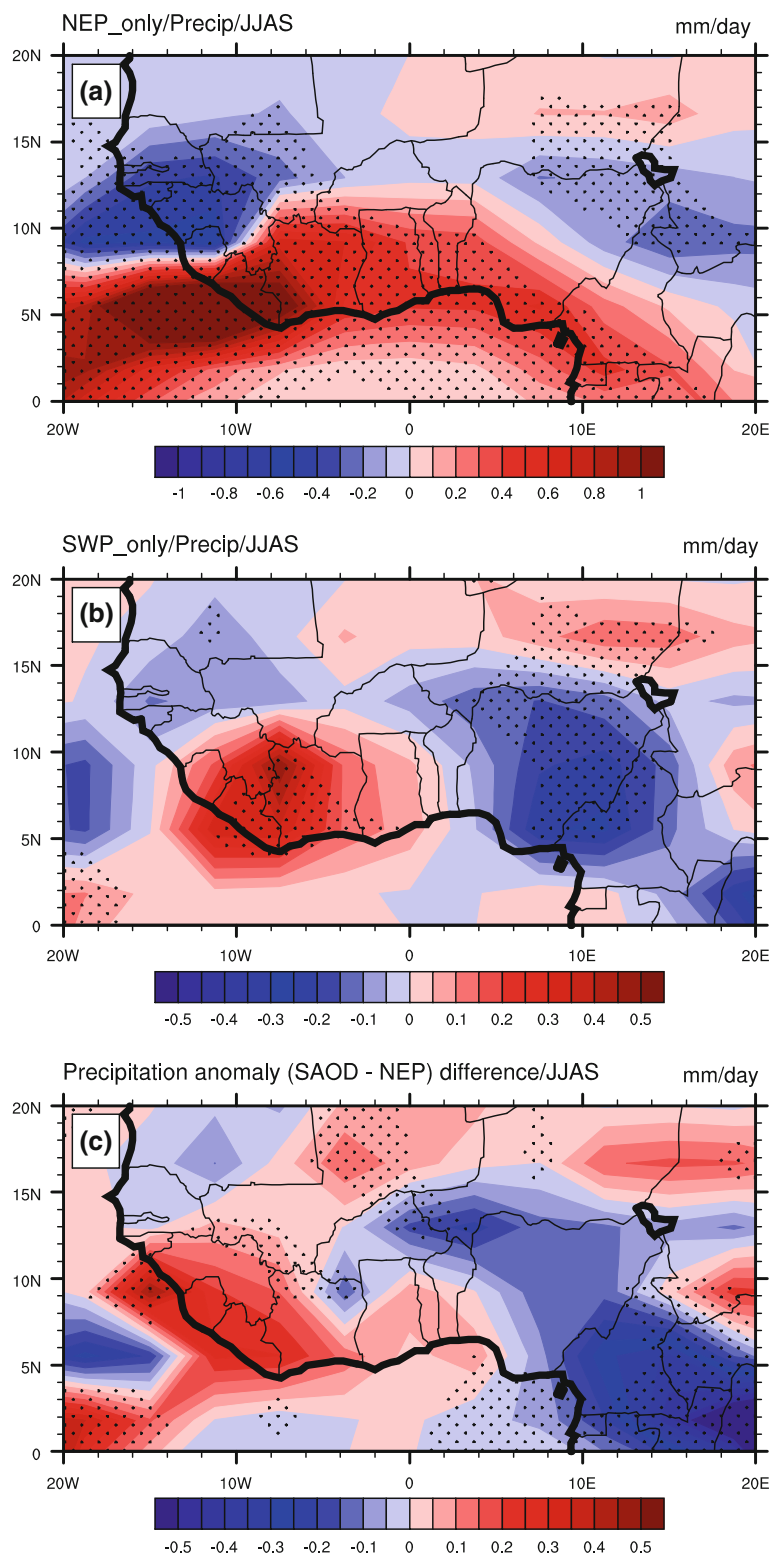
impacts of the NEP and then SWP. The well-known influence of the NEP/Gulf of Guinea/Atlantic Niño region on West Africa somewhat similar to the SAOD influence is reproduced in the *NEP-only experiment*. Thus, there are precipitation increases at most locations over the Guinea Coast, and decreases over the Sahel especially the western and eastern parts (Fig. 13a). Note however that most prominent Atlantic Niño cases co-occur with opposite anomalies in the extra-tropics (cf. Fig. 3) so that in reality, the effect of *Atlantic Niño only* SST variability on Guinea
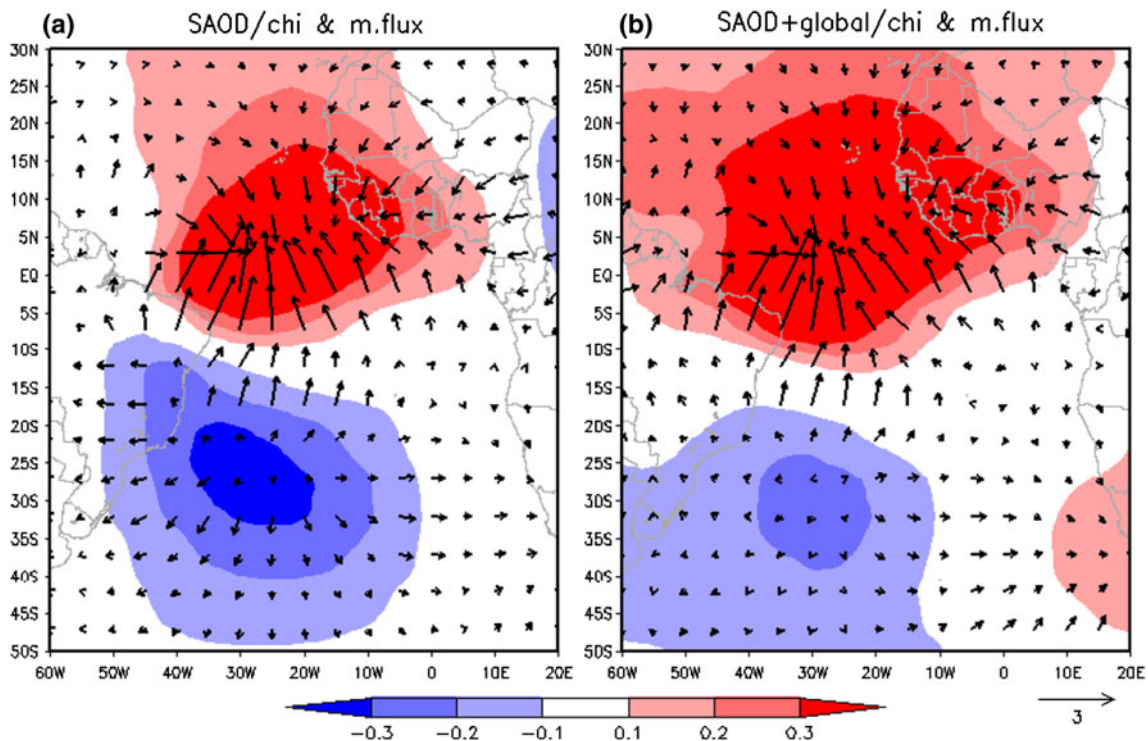
Fig. 14 Anomalous velocity potential averaged over the lower troposphere 925–400 hPa (*shading*: unit, 10^6 m²/s) for the *SAOD-only* (*left panel*) and *SAOD + global SSTA* (*right panel*) experiments. Vectors show the divergent component of the mass flux vertically integrated over the same layers (unit: kg m^{-1} s^{-1}). Both maps are based on the average of the positive and negative experiments

Coast precipitation may be far less than suggested by the simulation.

Of interest here is the precipitation anomalies simulated in the *SWP-only experiment* in which the climatological SST is prescribed elsewhere except the SAO where only *negative* SAOD-type SSTA is imposed (Fig. 13b). The simulation result is consistent with the full SAOD experiments in three aspects of interest here. One, there is positive response over the Guinea Coast from the west coast up to Benin Republic. Two, the mid-belt is characterized by negative precipitation anomalies, most marked on the west coast of the Sahel, and along the border of southeastern Nigeria and Cameroun. Three, above the average precipitation amounts are simulated in the northeastern part of the domain. Thus, it appears that the SWP indeed contributes to the precipitation anomalies, which with the inclusion of the NEP is greatly amplified and extends eastwards (cf. Fig. 7).

We further explore the interactions between the two centres of action in the SAO during SAOD that could affect Guinea Coast precipitation. Figure 14 shows the lower tropospheric averaged velocity potential and the divergent component of the vertically integrated mass flux. An anomalous vigorous upward motion occurs over a large area in the NEP/Atlantic Niño/Gulf of Guinea/West Africa region. Over the equatorial Atlantic Ocean, this is linked to a strong mass flux convergence a few orders of latitude to the north and along the coastal fringe of West Africa. On the other hand, at the SWP suppressed convection centred at 30°S, 30°W prevails and extends over a large domain. This gives rise to a strong mass divergence over the SWP. The occurrence of this pronounced opposite polarity creates a form of horizontal gradient by which mass diverging in the SWP region tends to boost the mass convergence, and then upward motion over the equatorial Atlantic Ocean.

This equatorial convergence plays important role in the generation of precipitation over the Guinea Coast. This is because within the SAOD context outlined, the SWP is a region of net mass deficit while the NEP is a region of net surplus. To account for this surplus, we have computed the vertically integrated moisture transport in the lower troposphere (Fig. 15). It readily can be seen that the western segment of the equatorial Atlantic Ocean of mass flux convergence is the major source of the moisture which undergoes westerly transport towards the Guinea Coast where it causes increases in precipitation.

As has been shown, the precipitation is largely limited to the Guinea Coast plausibly due to the oceanic/coastal nature of the deep convection and equatorial mass flux

Fig. 15 Anomalous moisture transport vertically integrated from in the lower troposphere from 925 to 400 hPa (vector: $1 \text{ g kg}^{-1} \text{ m s}^{-1}$). *Shading* indicates the magnitude of the moisture transport
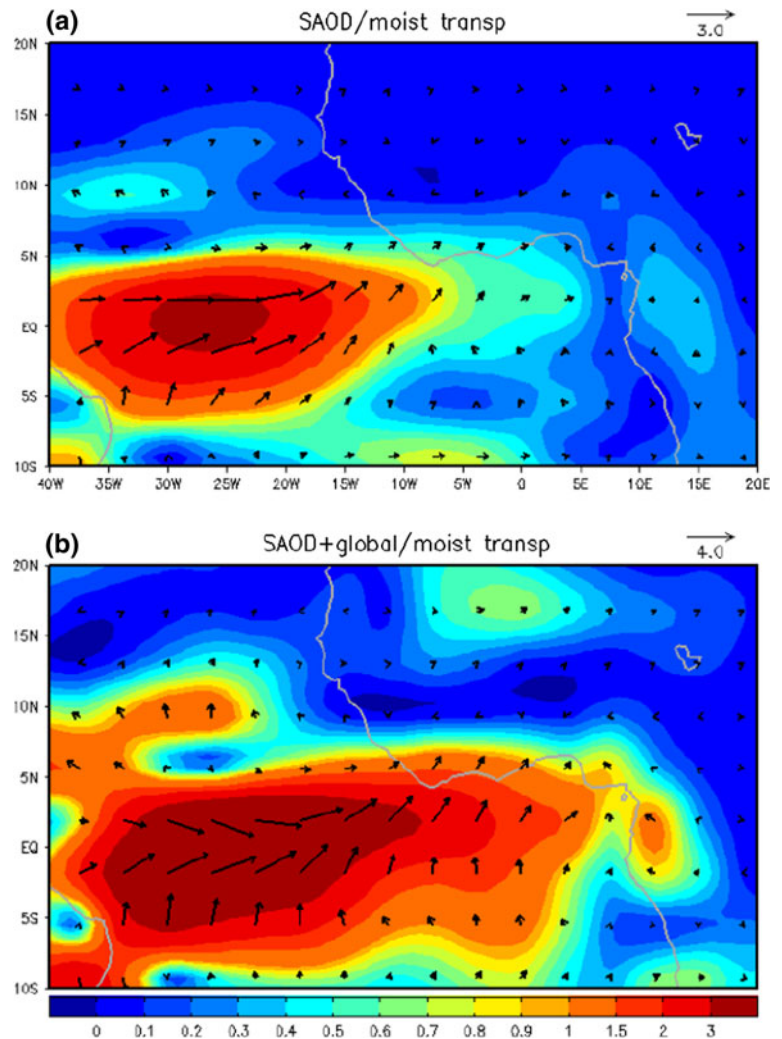

convergence field. As a result of this, the continental convergence associated with the West African summer monsoon (cf. Fig. 6) and therefore precipitation in the Sahel is weakened. We have also investigated the meridional circulation field to illustrate the tropospheric connection between the SWP and NEP vis-à-vis Guinea Coast precipitation. As shown in Fig. 16, there is a strong surface subsidence in the extra-tropics which tends to reinforce the upward motion in the NEP region. The vertical motion field exhibits great vertical extent up to 200 hPa where it subsides at the SWP to complete the loop. Indeed, the vertical motion in the NEP region is basically an equatorial phenomenon, and this explains why the precipitation impacts are basically restricted to the Guinea Coast.

4 Summary and concluding remarks

Based on the summer monsoon season (that is, June–July–August–September, JJAS) we have described in this paper,

the successful simulation of the impacts of the SAOD on Guinea Coast precipitation by prescribing idealized but realistic SAOD-type SSTA over the SAO in an intermediate complexity AGCM. The model generates significant precipitation anomalies over the Guinea Coast in the positive and negative phases of the dipole event, but the response in the Sahel further inland is rather weak. Above the average summer precipitation is associated with the positive SAOD episode in which warm SSTA occurs in the Gulf of Guinea and cool SSTA in the extra-tropics off the Brazil-Uruguay-Argentina coast. The reverse is also the case. Similar precipitation increases over the Guinea Coast were also reported in recent studies based on Atlantic Niño composites with weak cooling in the extra-tropics (Losada et al. 2010; Rodríguez-Fonseca et al. 2011).

We equally performed a second set of experiments in which global SSTA is prescribed with, and then without the SAOD-type SSTA in the SAO. It is found that the SAOD-type precipitation anomalies remain dominant in those simulations involving global SST variability if the SAOD
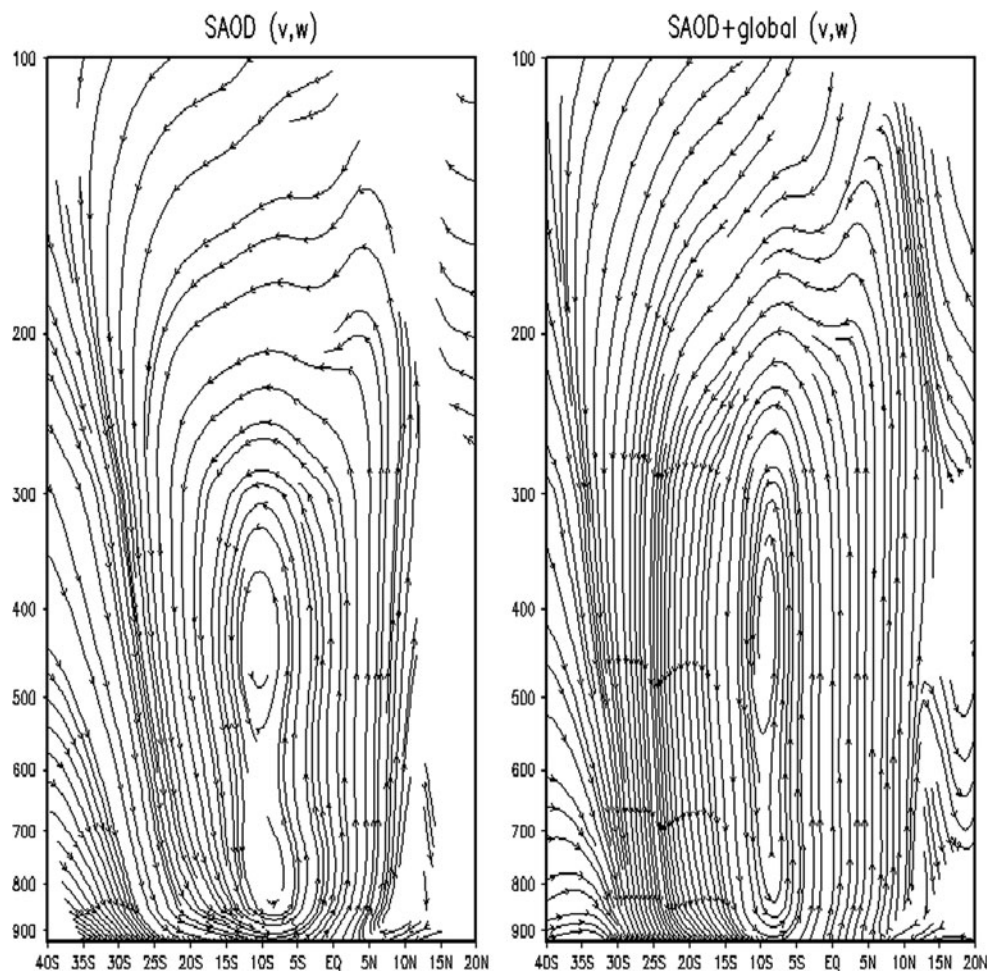
Fig. 16 Composite difference of Hadley circulation anomalies (averaged over 10°E–40°W) based on the *SAOD-only* (*left panel*) and *SAOD + global SSTA* (*right panel*) experiments

is present, but disappears in absence of the SAOD. These suggest that in active years the SAOD it constitutes a primary influence on the Guinea Coast precipitation. The impact of the global SST variability tends to strengthen the atmospheric response at the NEP/equatorial Atlantic region and consequently increase (reduce) the actual amount of precipitation received in the positive (negative) phase of the SAOD.

While the NEP/Gulf Guinea/Equatorial Atlantic/Atlantic Niño region is long known to influence Guinea Coast precipitation, of significance in this study is the role of the SWP in the extra-tropical SAO. This is confirmed by the robust response of the region's precipitation after the anomalous warming at the NEP is turned off in the model. It is shown that the interactions between the two centres of action of the SAOD determine its impacts Guinea Coast precipitation. Indeed, there is a growing body of literature emphasizing the dependency of the tropical Atlantic Ocean influence on West African precipitation on remote, extra-

tropical influences (e.g. Bader and Latif 2011; Fontaine et al. 2011; Rodríguez-Fonseca et al. 2011).

In the lower troposphere, there is deep convective motion over the equatorial Atlantic Ocean associated with large-scale mass flux convergence extending to the coastal fringes of West Africa. At the SWP, the anomalous cooling leads to suppressed convection, strong mass divergence and subsidence motion which amplifies the sub-tropical arm of the anomalous Hadley-type circulation. This tends to boost the mass convergence, uplift in the equatorial region and therefore enhanced precipitation at the Guinea Coast. A reversal of this mechanism (not described in details) could equally account to precipitation failure associated with the negative phase of the SAOD.

completed. With thank the anonymous reviewers for thorough criticisms of an earlier draft of this paper.

References

Adler RF, Huffman GJ, Chang A, Ferraro R, Xie P, Janowiak J, Rudolf B, Schneider U, Curtis S, Bolvin D, Gruber A, Susskind J, Arkin P (2003) The version 2 global precipitation climatology project (GPCP) monthly precipitation analysis (1979-present). J Hydrometeor 4:1147–1167

Bader J, Latif M (2011) The 1983 drought in the West Sahel: a case study. Clim Dyn 36:463–472

Biasutti M, Held IM, Sobel AH, Giannini A (2008) SST forcings and Sahel Rainfall variability in simulations of the twentieth and twenty-first centuries. J Clim 21:3471–3486

Bourke W (1974) A multilevel spectral model. I. Formulation and hemispheric integrations. Mon Wea Rev 102:687–701

Bulić IC, Kucharski F (2012) Delayed ENSO impact on spring precipitation over North/Atlantic European region. Clim Dyn 38:2593–2612

Charney J, Stone PH, Quirk WJ (1975) Drought in the Sahara: a biogeophysical feedback mechanism. Science 187:434–435

Colberg F, Reason CJC (2007) Ocean model diagnosis of low-frequency climate variability in the South Atlantic region. J Clim 20:1016–1034

De Xue Y, Sales F, Lau K-MW, Boone A, Feng J, Dirmeyer P, Guo Z, Kim K-M, Kitoh A, Kumar V, Poccard-Leclercq I, Mahowald N, Moufouma-Okia W, Pegion P, Rowell D, Schubert SD, Sealy A, Thiaw WM, Vintzileos A, Williams S, Wu M-LC (2010) Intercomparison and analyses of the climatology of the West AfricanMonsoon in the West African Monsoon modeling and evaluation project (WAMME) first model intercomparison experiment. Clim Dyn 35:3–27

Dee DP, Uppala SM, Simmons AJ et al (2011) The ERA-Interim reanalysis: configuration and performance of the data assimilation system. Q J R Meteorol Soc 137:553–597

Feng R, Li J, Wang J (2011) Regime change of the boreal summer Hadley circulation and its connection with the tropical SST. J Clim 24:3867–3877

Folland CK, Palmer TN, Parker DE (1986) Sahel rainfall and worldwide sea temperatures, 1901–85. Nature 320:602–607

Fontaine B, Trzaska S, Janicot S (1998) Evolution of the relationship between near global and Atlantic SST modes and the rainy season in West Africa: statistical analyses and sensitivity experiments. Clim Dyn 14:353–368

Fontaine B, García-Serrano J, Roucou P, Rodríguez-Fonseca B, Losada T, Chauvin F, Gervois S, Sivarajan S, Ruti P, Janicot S (2009) Impacts of warm and cold situations in the Mediterranean Basins on the West African monsoon: observed connection patterns (1979–2006) and climate simulations. Clim Dyn 35:95–114

Fontaine B, Gaetani M, Ullmann A, Roucou P (2011) Time evolution of observed July–September sea surface temperature-Sahel climate teleconnection with removed quasi-global effect (1900–2008). J Geophys Res 116:D04105. doi:10.1029/2010JD014843

Giannini A, Saravanan R, Chang P (2003) Oceanic forcing of Sahel Rainfall on interannual to interdecadal time scales. Science 302:1027–1030

Haarsma RJ, Campos EJD, Molteni F (2003) Atmospheric response to South Atlantic SST dipole. Geophys Res Lett 30:1864. doi:10.1029/2003GL017829

Haarsma RJ, Campos EJD, Hazeleger W, Severijns C, Piola AR, Molteni F (2005) Dominant modes of variability in the South Atlantic: a study with a hierarchy of ocean–atmosphere Models. J Clim 18:1719–1735

Held IM, Suarez MJ (1994) A proposal for the intercomparison of dynamical cores of atmospheric general circulation models. Bull Am Meteor Soc 75:1825–1830

Held IM, Delworth TL, Lu J, Findell KL, Knutson TR (2005) Simulation of Sahel drought in the 20th and 21st centuries. PNAS 102:17891–17896

Janowiak JE (1988) An Investigation of interannual rainfall variability in Africa. J Clim 1:240–255

Joly M, Voldoire A (2009) Influence of ENSO on the West African monsoon: temporal aspects and atmospheric processes. J Clim 22:3193–3210

Joly M, Voldoire A (2010) Role of the Gulf of Guinea in the interannual variability of the West African monsoon: what do we learn from CMIP3 coupled simulations? Int J Climatol 30:1843–1856

King MP, Kucharski F, Molteni F (2010) The roles of external forcings and internal variabilies in the northern hemisphere atmospheric circulation change from the 1960s to the 1990s. J Clim 23:6200–6220

Kucharski F, Molteni F, Bracco A (2006) Decadal interactions between the western tropical Pacific and the North Atlantic Oscillation. Clim Dyn 26:79–91

Kucharski F, Bracco A, Barimalala R, Yoo JH (2011) Contribution of the east–west thermal heating contrast to the South Asian Monsoon and consequences for its variability. Clim Dyn 37:721–735

Losada T, Rodriguez-Fonseca B, Janicot S, Gervois S, Chauvin F, Ruti P (2010) A multi-model approach to the Atlantic Equatorial mode: impact on the West African monsoon. Clim Dyn 35:29–43

Losada T, Rodriguez-Fonseca B, Mohino E, Bader J, Janicot S, Mechoso CR (2012) Tropical SST and Sahel rainfall: a non-stationary relationship. Geophys Res Lett 39:12. doi:10.1029/2012GL052423

Ma J, Li J (2008) The principal modes of variability of the boreal winter Hadley cell. Geophys Res Lett 35:L01808. doi:10.1029/2007GL031883

Mohino E, Rodrà-guez-Fonseca B, Mechoso CR, Gervois S, Ruti P, Chauvin F (2011) Impacts of the tropical Pacific/Indian oceans on the seasonal cycle of the West African monsoon. J Clim 24:3878–3891

Molteni F (2003) Atmospheric simulations using a GCM with simplified physical parameterizations. I. Model climatology and variability in multi-decadal experiments. Clim Dyn 20:175–191

Molteni F, King MP, Kucharski F, Straus DM (2011) Planetary-scale variability in the northern winter and the impact of land–sea thermal contrast. Clim Dyn 37:151–170

Nnamchi HC, Li J (2011) Influence of the South Atlantic Ocean dipole on West African summer precipitation. J Clim 24:1184–1197

Nnamchi HC, Li J, Anyadike RNC (2011) Does a dipole mode really exist in the South Atlantic Ocean? J Geophys Res 116:D15104. doi:10.1029/2010JD015579

Polo I, Rodríguez-Fonseca B, Losada T, García-Serrano J (2008) Tropical Atlantic variability modes (1979–2002). Part I: time evolving SST modes related to West African rainfall. J Clim 21:6457–6475

Robertson AW, Mechoso CR (2000) Interannual and interdecadal variability of the South Atlantic convergence zone. Mon Wea Rev 128:2947–2957

Rodríguez-Fonseca B, Janicot S, Mohino E, Losada T, Bader J, Caminade C, Chauvin F, Fontaine B, García-Serrano J, Gervois S, Joly M, Polo I, Ruti P, Roucou P, Voldoire A (2011) Interannual and decadal SST-forced responses of the West African monsoon. Atmos Sci Let 12:67–74

Shukla J (1998) Predictability in the midst of chaos: a scientific basis for climate forecasting. Science 282:728–731

Smith TM, Reynolds RW, Peterson TC, Lawrimore J (2008) Improvements to NOAA's historicalmerged land–ocean surface temperature analysis (1880–2006). J Clim 21:2283–2296

Taylor CM, Lambin EF, Stephenne N, Harding RJ, Essery RLH (2002) The Influence of land usechange on climate in the Sahel. J Clim 15:3615–3629

Trzaska S, Robertson AW, Farrara J, Mechoso CR (2007) South Atlantic variability arising from air-sea coupling: local mechanisms and tropical–subtropical interactions. J Clim 20:3345–3365

Uppala SM, KÅllberg PW, Simmons AJ et al (2005) The ERA-40 re-analysis. Q J R Meteorol Soc 131:2961–3012

Venegas SA, Mysak LA, Straub DN (1996) Evidence for interannual and interdecadal climate variability in the South Atlantic. Geophys Res Lett 23:2673–2676

Venegas SA, Mysak LA, Straub DN (1997) Atmosphere–ocean coupled variability in the South Atlantic. J. Climate 10:2904–2920

Vizy EK, Cook KH (2001) Mechanisms by which Gulf of Guinea and Eastern North Atlantic sea surface temperature anomalies can influence African Rainfall. J Clim 14:795–821

Wagner RG, Da Silva AM (1994) Surface conditions associated with anomalous rainfall in the Guinea coastal region. Int J Climatol 14:179–199

Xue Y, Shukla J (1993) The Influence of land surface properties on Sahel climate. Part 1: desertification. J Clim 6:2232–2245

Zamboni L, Kucharski F, Mechoso CR (2012) Seasonal variations of the links between the interannual variability of South America and the South Pacific. Clim Dyn 38:2115–2129

Zebiak SE (1993) Air–sea interaction in equatorial Atlantic region. J Clim 6:1567–1586